

A new insight into ethoxyquin fate in surface waters: Stability, direct and indirect photochemical behaviour and the identification of main products



Aziza Toure Bintou^{a,b}, Angelica Bianco^{a,b}, Gilles Mailhot^{a,b}, Marcello Brigante^{a,b,*}

^a Université Clermont Auvergne, Université Blaise Pascal, Institut de Chimie de Clermont-Ferrand, BP 10448, F-63000 Clermont-Ferrand, France

^b CNRS, UMR 6296, ICCF, F-63171 Aubiere, France

ARTICLE INFO

Article history:

Received 7 April 2015

Received in revised form 23 June 2015

Accepted 24 June 2015

Available online 27 June 2015

Keywords:

Environmental fate

Pollutant photochemistry

Surface water transformation

Polychromatic quantum yield

Pollutant lifetime

ABSTRACT

In this work, the fate of ethoxyquin (ETX), an antioxidant used as a food preservative and a pesticide, is investigated under ultraviolet and visible irradiation. The fast photolysis observed under environmentally closed conditions results in estimated degradation rates (R_{ETX}^d) of 1.6×10^{-8} and $8.7 \times 10^{-7} \text{ M s}^{-1}$ at pH 2.7 and 8.0, respectively. Under our experimental conditions, the polychromatic quantum yield (ϕ_{ETX}) is evaluated to be 5.0×10^{-3} and 1.4×10^{-1} for the protonated and anionic forms of ETX, respectively. The effect of hydroxyl radical on ETX degradation is evaluated, and the degradation kinetics profiles suggest that transformation via hydroxyl radical can be neglected compared with direct photolysis. Structures for the main degradation products (hydrolysis, photochemical and HO^\bullet -mediated derivative) are proposed. The kinetic parameters are used as inputs in APEX software to model the degradation of ETX as a function of different scenarios in surface waters. Finally, the irradiation of ETX under sun-simulated conditions estimates the life of this compound to be $\sim 38 \text{ s}$.

© 2015 Elsevier B.V. All rights reserved.

1. Introduction

The investigation of xenobiotic fate has received increasing attention in the last two decades due to their quantification in wastewaters and aquatic compartments [1–3]. Sun radiation is now considered as a key factor responsible for the transformation of pesticides and drugs via direct photolysis or the formation of transient species in surface waters [4,5].

Ethoxyquin (ETX) is an antioxidant used as a food preservative and a pesticide [6]. ETX is one of the most used antioxidants because it prevents the rancidification of fats in animal feed, especially at low temperatures, where the rate of decomposition of this product is low because the rate constant for the interaction of peroxy-radicals with ethoxyquin is significantly greater than the corresponding constant for fatty acids and because the product formed is relatively inactive [7]. ETX has been detected in paprika [8] and pears and apples [9]. Its main role is to prevent colour loss due to oxidation of the natural carotenoid pigments and to control scald (browning). ETX is not authorised in food production in Australia or within the European Union, but it is an accepted

additive in U.S.A. An ETX risk assessment was performed using a streamlined process for lower risk/exposure pesticide chemicals. Although the ETX toxicology database is not complete, it provides adequate information for evaluating and characterising the risks under the FIFRA (Federal Insecticide, Fungicide and Rodenticide Act) and FQPA (Food Quality protection Act), which were both released by the EPA (Environmental protection Agency) to limit the use of this chemical. ETX has low to moderate acute toxicity by oral (Category III), dermal (Category III) and inhalation (Category III) exposure routes. It is not an eye irritant (Category IV), and it produces minimal irritation to the skin (Category IV) [10]. Tests in animals show that ETX has a weak sensitizing potential; however, extensive human experience in using this chemical has indicated contact dermatitis, thus necessitating the discontinuation of working with ETX [10]. Although it has been approved for use in foods and as a spray insecticide for fruits, ETX has not been thoroughly tested for carcinogenic potential. ETX has been suggested that as a possible carcinogen because a very closely related chemical, 1,2-dihydro-2,2,4-trimethylquinoline, has been demonstrated to be carcinogenic in rats [11]. Although ETX was assessed to be slightly toxic to fish, it is commonly used as antioxidant in fish meal and fish oil to limit lipid oxidation. The highest levels of ETX (0.17 mg kg^{-1}) were found in farmed Atlantic salmon fillets [12], while the lowest concentrations of the

* Corresponding author.

E-mail address: marcello.brigante@univ-bpclermont.fr (M. Brigante).

synthetic antioxidant found were in cod. The concentration of the oxidation product ethoxyquin dimer (EQDM) was more than ten times higher than the concentration of parent ETX in Atlantic salmon, whereas this dimer was not detected in cod fillets [13]. The reactivity of ETX in natural waters is completely unknown. Despite its significant use in aquaculture, the environmental fate of ETX in aquatic environments has not been studied. In the present work, the transformation of ETX in water is investigated under sun-simulated conditions. The kinetic parameters obtained from steady-state irradiation are used to assess the life time of ETX under different physico-chemical conditions such as irradiation energy, hydroxyl radical concentration, water column depth and presence of organic matter.

2. Material and methods

2.1. Reagents

ETX was purchased from Fluka ($\geq 97.8\%$) and used as received. Analytical grade perchloric acid, sodium hydroxide, sodium nitrite were purchased from Prolabo. Terephthalic acid ($>99\%$) was purchased from Alfa Aesar. HPLC grade acetonitrile was obtained from VWR Prolabo. Ammonium acetate ($\geq 97\%$) was purchased from Fluka.

All solutions were prepared with distilled water purified by a Millipore system with a resistivity of $18 \text{ M}\Omega \text{ cm}$ and $\text{DOC} < 0.1 \text{ mg L}^{-1}$.

2.2. Solution preparation

ETX is weakly soluble (170 mg L^{-1}) [16] in water and the UV–vis spectrum of ETX solution ($1 \times 10^{-4} \text{ M}$) shows a time evolution if kept in the dark at room temperature (Fig. SM1). Therefore stability of ETX in acetonitrile was tested and any notably modification was observed after 1 week in dark. For these reasons, a concentrated stock solution ($2 \times 10^{-3} \text{ M}$) in acetonitrile (solubility of 462 g L^{-1}) was stored in the dark, and fresh solutions were prepared just before irradiation by diluting aliquots in Milli-Q water (approximately 2% acetonitrile by volume) to obtain the desired concentration ($5 \times 10^{-5} \text{ M}$).

2.3. Irradiation procedures

Irradiation was performed using a homemade irradiation system placed in a cylindrical stainless-steel container equipped with six fluorescent lamps (Philips TL D15W/05) with emission spectra ranging from 300 to 500 nm. The photoreactor, a Pyrex tube with an internal diameter of 2.6 cm, was placed in the centre of the setup. The total solution volume was 50 mL, and all experiments were carried out at room temperature ($293 \pm 2 \text{ K}$). Samples were taken from the reaction tube at fixed interval times. The emission spectrum of the irradiation system with two lamps (Fig. 1) was recorded using fibre optics coupled with a charge-coupled device (CCD) spectrophotometer (Ocean Optics USD 2000+UV–vis) and normalised using a PNA/pyridine actinometer method [14]. The photon flux reaching the solution (I_a) was estimated using Eq. (1):

$$I_a = \frac{\Delta N_{\text{PNA}}}{\phi^{\text{PNA}}} \quad (1)$$

where ΔN_{PNA} represents the amount of PNA decomposed and ϕ^{PNA} , the photodegradation quantum yield, is calculated using the relation $\phi^{\text{PNA}} = 0.44 \times [\text{pyridine}] + 0.00028$. Using 0.1 mM of pyridine ϕ^{PNA} was calculated to be 3.24×10^{-4} .

The total irradiance between 300 and 500 nm reaching the solution was then estimated to be between 3.5 and 20.8 W cm^{-2} (corresponding to 0.67 and $4.01 \times 10^{19} \text{ photons cm}^{-2} \text{ s}^{-1}$) using one and six lamps, respectively.

Solutions were doped with hydrogen peroxide (H_2O_2) and nitrate (NO_3^-) in order to generate hydroxyl radical under irradiation. Both compounds are chosen because they are naturally occurring compounds generally found in surface and/or atmospheric waters and due to low reactivity with photogenerated hydroxyl radical (i.e. generally not considered as HO^\bullet scavengers).

2.4. UV–vis and fluorescence spectroscopy

Solution absorbance was determined using a Varian Cary 300 Scan UV–vis double beam spectrophotometer, while hydroxyl radical formation rate was determined using a terephthalic acid chemical probe by the method previously described by Charbouillot et al. [15]. The formation of hydroxyterephthalic acid was quantified using a Varian Cary Eclipse fluorescence spectrophotometer with an excitation wavelength (λ_{ex}) of 320 nm and an

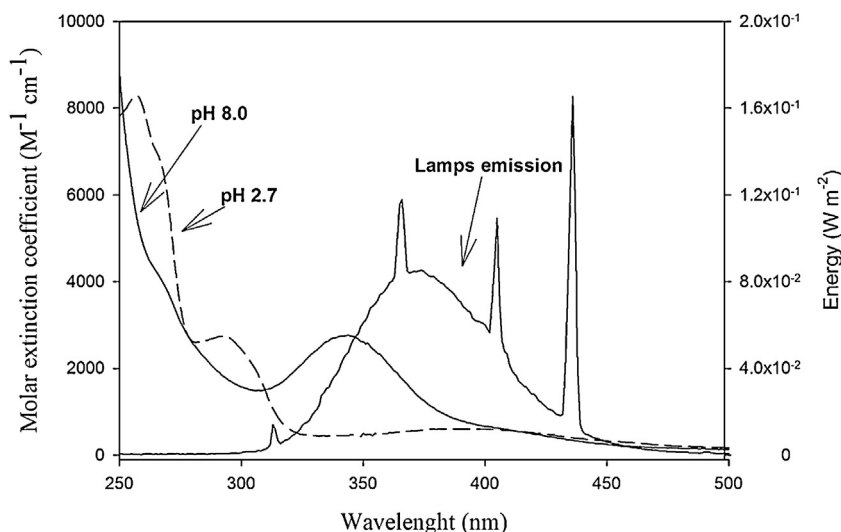


Fig. 1. UV–vis spectra of ETX at pH 2.7 (protonated form) and pH 8.0 (anionic form) and emission spectrum for the irradiation system with two lamps.

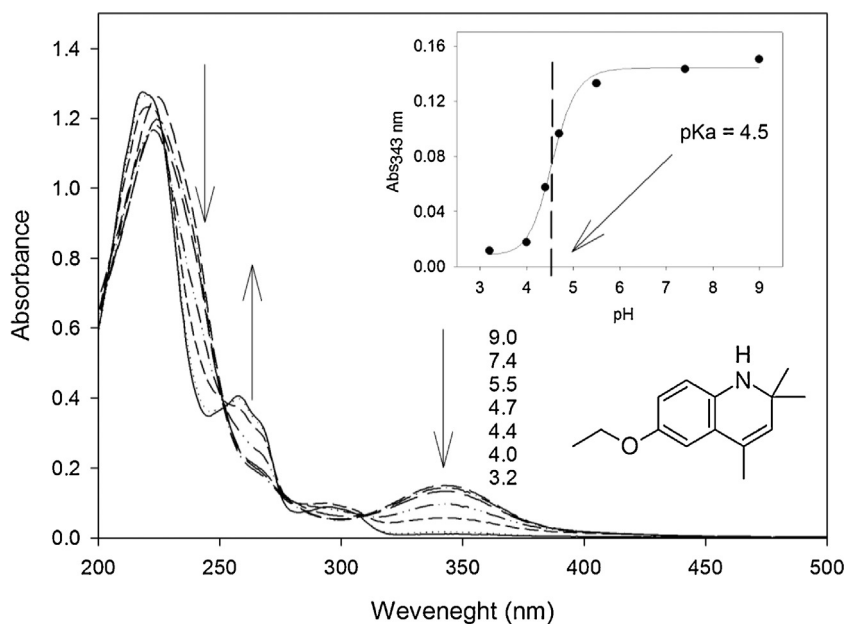


Fig. 2. Evolution of the ethoxyquin UV-vis spectrum as a function of pH. Inset: chemical structure of ETX and Abs at 343 nm as a function of pH.

emission wavelength (λ_{em}) of 420 nm. The scan rate and bandpass were 600 nm min^{-1} and 10 nm , respectively, for both excitation and emission.

2.5. Liquid chromatography

ETX concentration was determined using a Water Acquity Ultra Performance LC instrument equipped with a Water Acquity Photo Diode Array detector and fluorescence detector. Compound separation was performed using a Water Acquity UPLC C18 ($100 \text{ mm} \times 2.1 \text{ mm} \times 1.7 \mu\text{m}$) column with isocratic elution (40% 0.01 M ammonium buffer and 60% acetonitrile) and an eluent flow rate of 0.3 mL min^{-1} . The ETX retention time under these conditions was 3.0 min. UV-vis detection was performed at $\lambda = 223 \text{ nm}$.

The chemical structures of ETX transformation products were proposed based on HPLC (Agilent 1100 Series, binary pump)

equipped with an ESI ion source (positive ion mode) and TOF and UV detectors. The adopted column was a Sphere Clone C18 (Phenomenex, $4.6 \times 250 \text{ mm} \times 5 \mu\text{m}$), and the gradient elution was as follows: initially 5% acetonitrile and 95% water-formic acid 1%; a linear gradient to 95% acetonitrile within 22 min; constant conditions for 20 min. The flow rate was 0.4 mL min^{-1} , and the UV detector was set at 254 nm .

2.6. Kinetic treatment of the data

The initial rates of ETX degradations were determined by fitting the experimental data with the pseudo-first order decay equation of the form $[\text{ETX}]_t = [\text{ETX}]_0 \exp(-k_{\text{ETX}}^d t)$, where $[\text{ETX}]_0$ and $[\text{ETX}]_t$ are the concentrations of ETX at the initial time at time t , respectively, and k_{ETX}^d is the pseudo-first decay constant. The degradation of ETX ($R_{\text{ETX}}^d, \text{M s}^{-1}$) could then be obtained from $k_{\text{ETX}}^d \times [\text{ETX}]_0$.

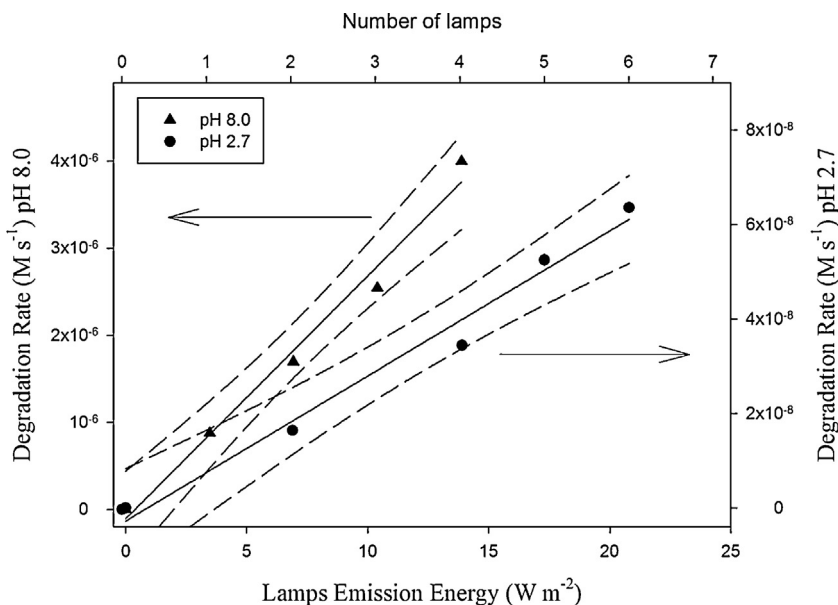


Fig. 3. Correlation between ETX degradation rates and irradiation energy between 290 and 500 nm at pH 2.7 and 8.0. Dashed lines denote the 95% confidence of the linear fit.

Table 1

Degradation rates of ETX (R_{ETX}^d) at pH 2.7 and 8.0 using different nitrite concentrations in the presence or absence of chloride. The errors are derived at the 1 σ level from the scattering of the data using an exponential decay fit.

pH 2.7	R_{ETX}^d (M s ⁻¹)	pH 8.0	R_{ETX}^d (M s ⁻¹)
ETX photolysis	$1.64 \pm 0.06 \times 10^{-8}$	ETX photolysis	$8.67 \pm 0.33 \times 10^{-7}$
10 μM $[\text{NO}_2^-]$	$2.25 \pm 0.03 \times 10^{-8}$	50 μM $[\text{NO}_2^-]$	$1.05 \pm 0.03 \times 10^{-6}$
20 μM $[\text{NO}_2^-]$	$3.66 \pm 0.04 \times 10^{-8}$	50 μM $[\text{NO}_2^-]$ + 0.5 M Cl^-	$1.12 \pm 0.06 \times 10^{-6}$
30 μM $[\text{NO}_2^-]$	$5.20 \pm 0.03 \times 10^{-8}$		
10 μM $[\text{NO}_2^-]$ + 0.5 M Cl^-	$1.53 \pm 0.15 \times 10^{-7}$		
20 μM $[\text{NO}_2^-]$ + 0.5 M Cl^-	$5.78 \pm 0.25 \times 10^{-7}$		

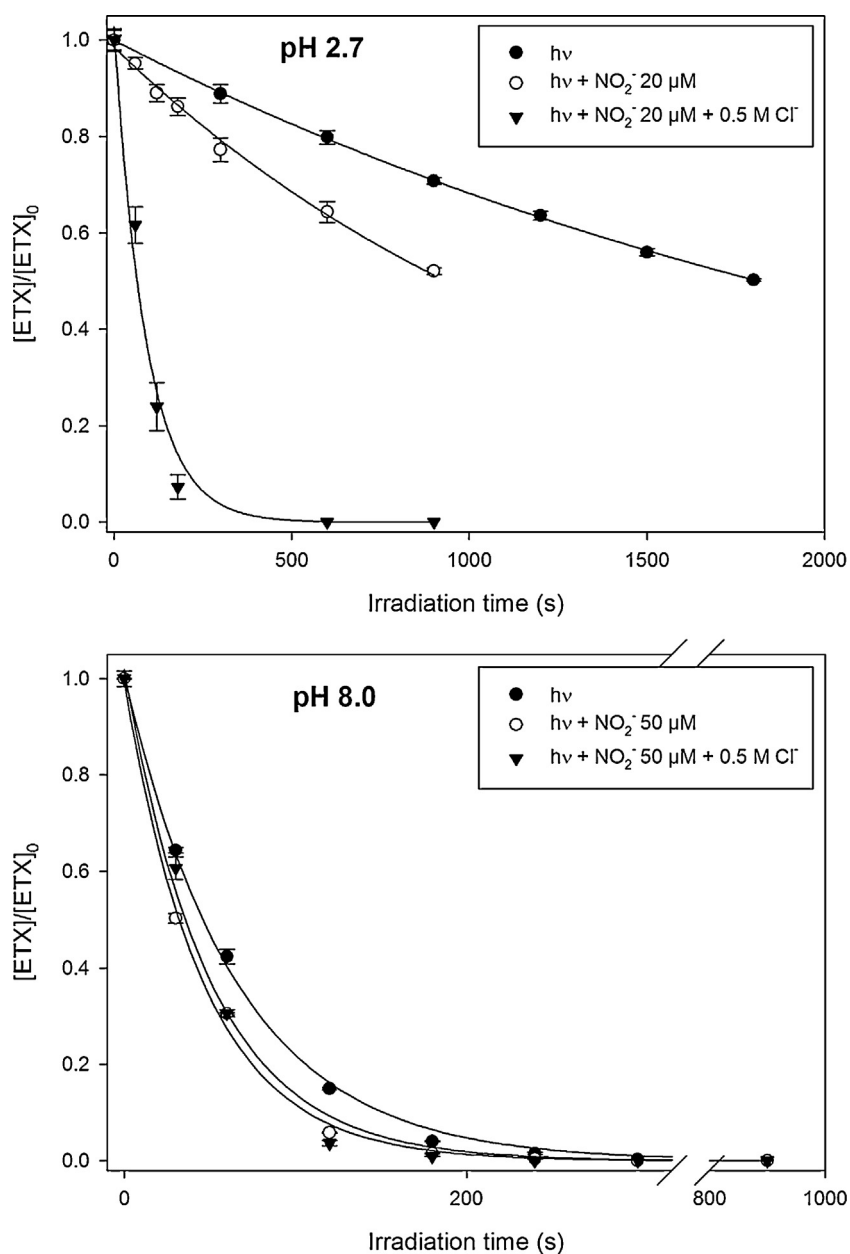


Fig. 4. Concentration evolution vs. irradiation time of ETX at pH 2.7 and 8.0 under direct photolysis and in the presence of nitrite and chloride. Solid lines are the exponential decay fits of the experimental data.

Half-life times ($t_{1/2}$) are evaluated considering the first order rate constant (k_{ETX}^d) of ethoxyquin and using Eq. (2)

$$t_{1/2} = \frac{\ln(2)}{k_{\text{ETX}}^d} \quad (2)$$

To compare the photodegradation efficiency at pH 2, 7 and 8.0, the polychromatic quantum yield between 300 and 500 nm was calculated ($\phi_{300-500\text{nm}}^{\text{ETX}}$). $\phi_{300-500\text{nm}}^{\text{ETX}}$ is defined as the ratio between the numbers of transformed molecules and the numbers of photons absorbed by solution (Eq. (3)):

$$\phi_{300-500\text{nm}}^{\text{ETX}} = \frac{R_{\text{ETX}}^d}{I_a} \quad (3)$$

where R_{ETX}^d is the ETX degradation rate (Ms^{-1}) and I_a is the absorbed photon flux per unit of surface and unit of time. The latter was calculated from Eq. (4):

$$I_a = \int_{\lambda} I_0(\lambda)(1 - 10^{-\varepsilon(\lambda)d[\text{ETX}]}) \quad (4)$$

where I_0 is the incident photon flux, ε the molar absorption coefficient of ETX, d the optical path length inside the cells and $[\text{ETX}]$ the initial ETX concentration.

Table 2

Degradation product identification for ETX under direct (photolysis) and indirect (HO^\bullet -mediated) photochemical conditions. R_t denotes the retention time using the HPLC conditions reported in the materials and methods section. $[\text{M} + \text{H}]^+$ is the HPLC-MS molecular peak for the reported irradiation conditions under which the molecule was detected.

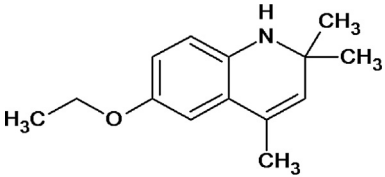
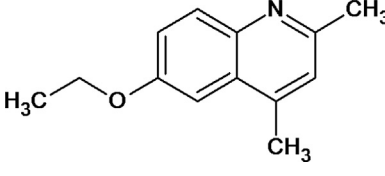
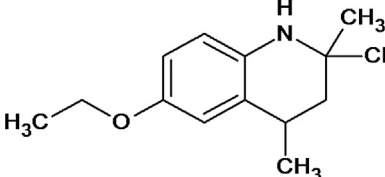
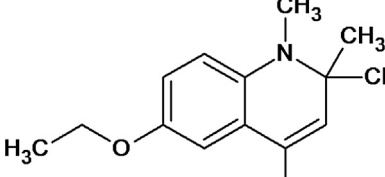
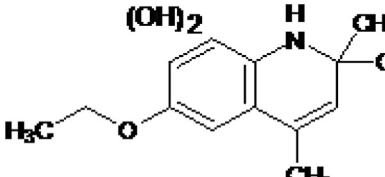
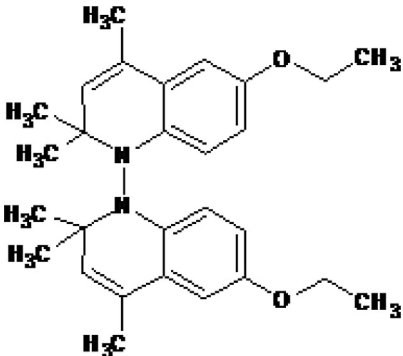
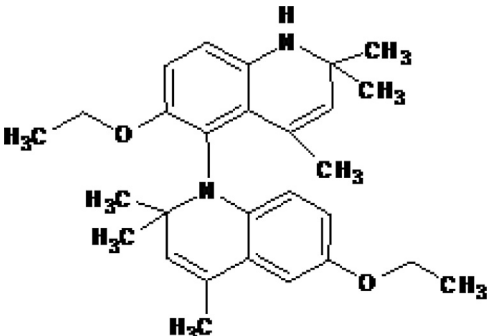
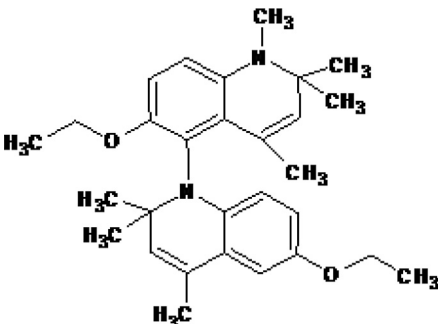
R_t (min)	$[\text{M} + \text{H}]^+$	Fragments	Conditions	Structure
6.7	218			 <p style="text-align: center;">ETX</p>
8.6	203	178, 167, 138	Hydrolysis and direct photolysis	 <p style="text-align: center;">ETX</p>
9.5	220	202, 173, 167	Direct photolysis	
12.2	233	173	Hydrolysis, direct photolysis,	
13.4	252	236, 214	Indirect Photolysis hydroxyl radical	

Table 2 (Continued)

R_f (min)	$[M+H]^+$	Fragments	Conditions	Structure
21.6	433		Direct photolysis	
22	448		Direct photolysis	
				

3. Results and discussion

3.1. Kinetic study

ETX is weakly soluble (170 mg L^{-1}) [16] in water, and a fresh $1 \times 10^{-4} \text{ M}$ solution of ETX kept in the dark at room temperature shows a notably modified UV–vis spectrum (Fig. SM1). For these reasons, a stock $2 \times 10^{-3} \text{ M}$ solution of ETX in acetonitrile (solubility of 462 g L^{-1}) was stored in the dark, and fresh solutions were prepared just before irradiation by diluting aliquots in Milli-Q water (approximately 2% acetonitrile by volume) to obtain a $5 \times 10^{-5} \text{ M}$ solution. Fig. 2 shows the absorption spectra of $5 \times 10^{-5} \text{ M}$ aqueous solutions of ETX at different pH values. The inset in Fig. 2 shows the variation in absorbance at 343 nm (Abs_{343}) as a function of pH. The Abs_{343} increases as pH increases from 3 to 5 and then reaches a plateau at higher pH values. An inflection point corresponding to the pK_a of the molecules can be observed around pH 4.5, in agreement with the literature data [17]. The deprotonated form of ETX absorbs in a much wider domain (200–

400 nm) than the acidic form (200–320 nm), as seen in Fig. 1, which shows the spectral overlap with the spectral emissions of the adopted lamps. ETX presents two absorption maxima at 223 nm and 343 nm.

Before irradiation experiments, the stability of ETX was tested in the dark; degradation due to hydrolysis and thermal effects is negligible during the adopted irradiation time (i.e. a few minutes).

ETX was irradiated at pH 2.7 (protonated form) and pH 8.0 (ionic form) using different numbers of lamps (corresponding to different irradiation energies; Fig. 3). A linear correlation is found between lamp energy (L_E , W m^{-2}) and ETX degradation rate (R_{ETX}^d). The R_{ETX}^d values were $3.07 \pm 0.25 \times 10^{-9} L_E$ and $2.78 \pm 0.20 \times 10^{-7} L_E$ for pH 2.7 and 8.0, respectively.

The polychromatic degradation quantum yield of ETX between 300 and 500 nm ($\phi_{300-500\text{nm}}^{\text{ETX}}$) can be estimated to be $5.03 \pm 0.03 \times 10^{-3}$ and $1.40 \pm 0.19 \times 10^{-1}$ at pH 2.7 and 8.0, respectively. Under the adopted irradiation conditions, the corresponding half-life time ($t_{1/2}$) can be evaluated as 30.1 min and 38 s at pH 2.7 and 8.0,

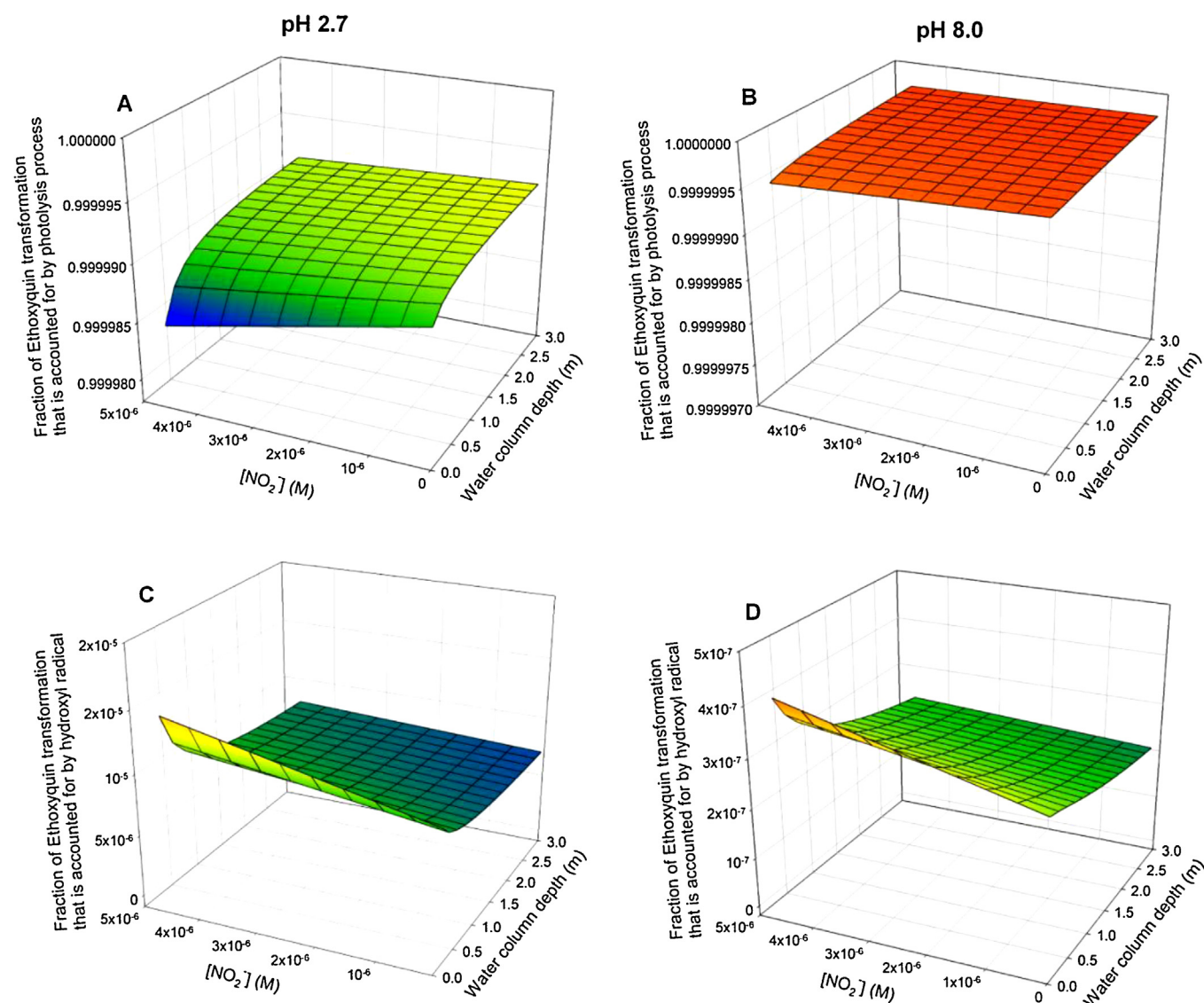


Fig. 5. Modelled fraction of ETX degradation attributed to direct photolysis and hydroxyl radical reactivity as a function of nitrite concentration and water column depth at pH 2.7 and 8.0.

respectively. At pH 2.7, the degradation rate of ETX under photolysis $R_{\text{ETX}}^{\text{d}}$ is $1.64 \pm 0.06 \times 10^{-8} \text{ M s}^{-1}$; the degradation rate is enhanced two-fold with the addition of $20 \mu\text{M}$ of NO_2^- (Table 1) due to the formation of hydroxyl radical (R1). In the presence of chloride, ETX is completely degraded after $\sim 250 \text{ s}$ (Fig. 4).

At pH 8.0, degradation under direct photolysis occurs much faster, but no significant differences are measured in the presence of nitrite and chloride, suggesting that the degradation of the anionic form of ETX can be ascribed exclusively to direct phototransformation.

This reactivity in acidic conditions can be explained considering that nitrite is a photochemical source of hydroxyl radical (R1), and nitrite acts as a scavenger hydroxyl radical ($k_{\text{NO}_2^-, \text{HO}^\bullet} = 1.2 \times 10^{10} \text{ M}^{-1} \text{ s}^{-1}$; R2) via electron transfer reaction.



In the presence of chloride in acidic conditions, photogenerated hydroxyl radical leads to the generation of dichloride radical anion

($\text{Cl}_2^{\bullet-}$) ($k_{\text{Cl}^-, \text{HO}^\bullet} = 3.0 \times 10^9 \text{ M}^{-1} \text{ s}^{-1}$; R3) which is also scavenged by nitrite ($k_{\text{NO}_2^-, \text{Cl}_2^{\bullet-}} = 2.5 \times 10^8 \text{ M}^{-1} \text{ s}^{-1}$; R4), but with a much smaller (around two orders of magnitude) rate constant compared with the scavenging of HO^\bullet .



Considering $20 \mu\text{M}$ of nitrite as a hydroxyl radical source and $R_{\text{NO}_2^-}^{\text{d, ETX}}$, the ETX degradation rates in the absence and presence of 0.5 M of chloride and the fraction of HO^\bullet reacting with nitrite can be evaluated by the following equation:

$$f_{\text{NO}_2^-}^{\text{HO}^\bullet} = 1 - \frac{R_{\text{NO}_2^- + \text{Cl}^-}^{\text{d, ETX}}}{R_{\text{NO}_2^-}^{\text{d, ETX}}} \quad (\text{5})$$

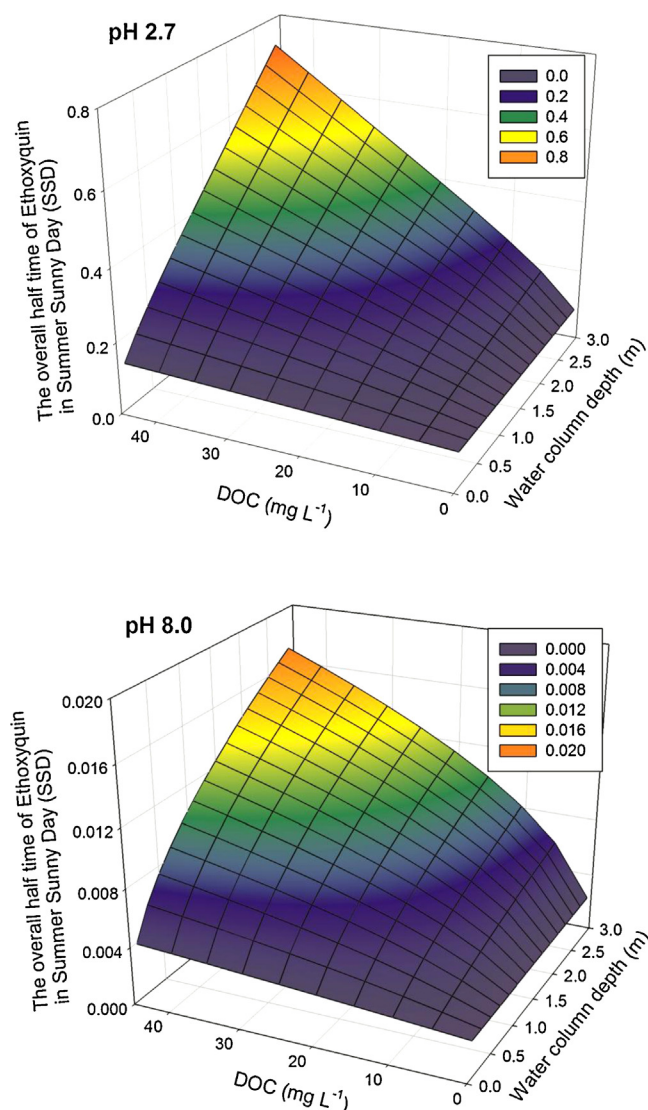


Fig. 6. Half-life time of ETX expressed as a fraction of solar sunny days (SSD) as a function of DOM concentration and water column depth at pH 2.7 and 8.0.

Eq. (5) can also be expressed as:

$$f_{\text{NO}_2^-, \text{HO}^\bullet}^{\text{HO}^\bullet} = \frac{k_{\text{NO}_2^-, \text{HO}^\bullet} [\text{NO}_2^-]}{k_{\text{NO}_2^-, \text{HO}^\bullet} [\text{NO}_2^-] + k_{\text{ETX}, \text{HO}^\bullet} [\text{ETX}]} \quad (6)$$

where $k_{\text{NO}_2^-, \text{HO}^\bullet}$ and $k_{\text{ETX}, \text{HO}^\bullet}$ are the second order rate constants of HO^\bullet with nitrite and ETX, respectively, and $[\text{NO}_2^-]$ and $[\text{ETX}]$ are their initial concentrations.

Combining Eq. (5) with Eq. (6), we can estimate the $k_{\text{ETX}, \text{HO}^\bullet}$ to be $4.7 \times 10^8 \text{ M}^{-1} \text{ s}^{-1}$ at pH 2.7. At pH 8.0, the hydroxyl radical reaction with chloride does not lead to the formation of chloride radical and dichloride radical anion [18]. Thus, as shown in Fig. 4, the effect of OH^\bullet -mediated ETX degradation can be considered to be negligible compared with direct phototransformation.

3.2. Product identification

Different irradiated ETX solutions were analysed by HPLC-MS, and the chemical structures of main transformation products are proposed in Table 2.

6-Ethoxy-2,4-dimethylquinoline is quantified as a degradation product in both hydrolysis and photolysis processes. The

formation of this product is attributed to the generation of N-radicals and the subsequent loss of methyl radical.

The main pathways for hydrolysis and photolysis are demethylation, with $[\text{M} + \text{H}]^+ = 202$, and methylation, with $[\text{M} + \text{H}]^+ = 233$. The concentrations of these products increase with irradiation time. Dimer production, which is known to occur during photolysis, is observed with $[\text{M} + \text{H}]^+ = 433$ at a retention time of 21.6 min [19].

The degradation of ETX was also performed in the presence of H_2O_2 as a photochemical source of HO^\bullet . Thus, the ETX solution was irradiated in the presence of $2 \times 10^{-3} \text{ M}$ hydrogen peroxide at pH 8.0 and analysed by mass spectrometry after 20 min of irradiation. Under such conditions, only dihydroxylated ETX products are found, with $[\text{M} + \text{H}]^+$ of 252.

3.3. Modelling fate in natural waters

The photoreactivity of ETX in surface waters upon irradiation (photolysis) and reaction with hydroxyl radicals was modelled by using the *savetable* function of APEX [20].

The fractions of ETX transformation due to photolysis and hydroxyl radical-mediated transformation was estimated at pH 2.7 and 8.0 (Fig. 5). Under both pH conditions, photolysis is the main pathway of ETX degradation (Fig. 5A and B), and the concentration of nitrite (a source of hydroxyl radical) and water column depth have no significant effect on ETX disappearance. The negligible influences of the presence of hydroxyl radical and water column depth are confirmed in Fig. 5C and D. In fact, the main photochemical sources of hydroxyl radicals in natural waters are nitrate and nitrite. In this work, the reactivity of ETX with HO^\bullet was investigated using different concentrations of nitrite. ETX photo-transformation by hydroxyl radical would plausibly be enhanced by increasing the concentration of nitrite. Fig. 5C and 5D show the fraction of ETX transformation attributed to hydroxyl radicals (on a scale from 0 to 1), indicating that the contribution of hydroxyl radical reactivity is negligible (<1%) for both the acidic and basic forms of ETX.

The total half-life time of ETX can be evaluated considering that the reverse of total half-life time is given by the sum of the reverse half-life time for each reaction. Thus, ETX half-life time ($t_{1/2}(\text{ETX})_{\text{tot}}$) can be estimated using Eq. (7):

$$\frac{1}{t_{1/2}(\text{ETX})_{\text{tot}}} = \frac{1}{t_{1/2}(\text{ETX})_{\text{HO}^\bullet}} + \frac{1}{t_{1/2}(\text{ETX})_{\text{hv}}} \quad (7)$$

where $t_{1/2}(\text{ETX})_{\text{HO}^\bullet}$ and $t_{1/2}(\text{ETX})_{\text{hv}}$ are the half-life times of ETX in the presence of hydroxyl radical and under photolysis, respectively.

Eq. (7) can be rearranged to give:

$$t_{1/2}(\text{ETX})_{\text{tot}} = \frac{t_{1/2}(\text{ETX})_{\text{HO}^\bullet} \times t_{1/2}(\text{ETX})_{\text{hv}}}{t_{1/2}(\text{ETX})_{\text{HO}^\bullet} + t_{1/2}(\text{ETX})_{\text{hv}}} \quad (8)$$

Fig. 6 shows the ETX half-life time as a function of dissolved organic matter (DOM) concentration (generally indicated in mg of carbons per litres and indicated with DOC abbreviation) concentration and the optical path length of sunlight in water, which can be considered the main parameters influencing the half-life time of organic compounds present in aquatic compartments. The modelling study results are expressed as half-life times on summer-sunny days (SSD) at pH 2.7 and 8.0. Two main effects were modelled: the water column depth and the DOC concentration. High DOC values lead to three main effects: (i) high scavenging of hydroxyl radicals; (ii) the production of reactive species by excited state of organic matter; and (iii) a decrease in the diffusion of light in the water column [21]. In the case of ETX, for which the photolysis reaction is the most significant degradation

pathway, the main effect of DOC is to decrease the diffusion of light throughout the water column. At pH 2.7, the half-life time of ETX ranges from 2 h at the water surface (with a negligible effect of DOC) to 0.8 SSD. For the anionic form of ETX (pH 8.0), which is expected to be the most relevant form in natural waters, the half-life time ranges from 4 min (at the surface with low DOM concentration) to 25 min (at a depth of 3 m with high DOM concentration).

4. Conclusions

In this work, we investigate for the first time, to the best of our knowledge, the fate of ETX in natural waters considering the photolysis process and HO[•]-mediated transformation for the first time. The deprotonated form of ETX, which is expected to be the primary form in natural waters, presents a life-time of a few minutes; thus, the quantification of this pesticide in natural waters is quite difficult.

Irradiation products are identified, and photolysis quantum yields are calculated under polychromatic irradiation (UVA and visible regions). This study could facilitate future research on the toxicity of photogenerated products, which are more capable of accumulating in the water body and thus in living organisms

Acknowledgements

The authors acknowledge financial support from the “Fédération des Recherches en Environnement” through the CPER “Environnement” founded by the “Re’gion Auvergne,” the French government and FEDER from the European Community.

Appendix A. Supplementary data

Supplementary data associated with this article can be found, in the online version, at <http://dx.doi.org/10.1016/j.jphotochem.2015.06.030>.

References

- [1] M. Kock-Schulmeyer, M. Villagrasa, M. Lopez de Alda, R. Cespedes-Sanchez, F. Ventura, D. Barcelo, Occurrence and behavior of pesticides in wastewater treatment plants and their environmental impact, *Sci. Total Environ.* 458–460 (1996) 466–476.
- [2] I.K. Konstantinou, D.G. Hela, T.A. Albanis, The status of pesticide pollution in surface waters (rivers and lakes) of Greece. Part I. Review on occurrence and levels, *Environ. Pollut.* 141 (2006) 555–570.
- [3] Y. Luo, W. Guo, H.H. Ngo, L.D. Nghiem, F.I. Hai, J. Zhang, S. Liang, X.C. Wang, A review on the occurrence of micropollutants in the aquatic environment and their fate and removal during wastewater treatment, *Sci. Total Environ.* 473–474 (2014) 619–641.
- [4] E. De Laurentiis, C. Prasse, T.A. Ternes, M. Minella, V. Maurino, C. Minero, M. Sarakha, M. Brigante, D. Vione, Assessing the photochemical transformation pathways of acetaminophen relevant to surface waters: transformation kinetics, intermediates, and modelling, *Water Res.* 53 (2014) 235–248.
- [5] F. Cermola, M. DellaGreca, M.R. Ilesce, S. Montanaro, L. Previtera, F. Temussi, M. Brigante, Irradiation of fluvastatin in water: structure elucidation of photoproducts, *J. Photochem. Photobiol. A* 189 (2007) 264–271.
- [6] T.A. Unger, *Ethoxyquin, Pesticide Synthesis Handbook*, William Andrew Publishing, Park Ridge, NJ, 1996586.
- [7] M.N. Emanuel, Chemical and biological kinetic, *Russ. Chem. Rev.* 50 (1981) 901–947.
- [8] P. Vinas, M.H. Cordoba, C. Sanchez-Pedreno, Determination of ethoxyquin in paprika by high-performance liquid chromatography, *Food Chem.* 42 (1991) 241–251.
- [9] Y. Pico, M. I. Farré, R. Segarra, D. Barcelo, Profiling of compounds and degradation products from the postharvest treatment of pears and apples by ultra-high pressure liquid chromatography quadrupole-time-of-flight mass spectrometry, *Talanta* 81 (2010) 281–293.
- [10] <http://www.epa.gov/pesticides/reregistration/REDs/factsheets/0003fact.pdf>.
- [11] Food Safety Commission of Japan, Risk Assessment Report Ethoxyquin, (2013).
- [12] A.K. Lundebye, H. Hove, A. Mage, V.J.B. Bohne, K. Hamre, Levels of synthetic antioxidants (ethoxyquin, butylated hydroxytoluene and butylated hydroxyanisole) in fish feed and commercially farmed fish, *Food Addit. Contam.* 27 (2010) 1652–1657.
- [13] P. He, R.G. Ackman, Residues of ethoxyquin and ethoxyquin dimer in ocean-farmed salmonids determined by high-pressure liquid chromatography, *J. Food Sci.* 65 (2000) 1312–1314.
- [14] D. Dulin, T. Mill, Development and evaluation of sunlight actinometers, *Environ. Sci. Technol.* 16 (1982) 815–820.
- [15] T. Charbouillot, M. Brigante, G. Mailhot, P.R. Maddigapu, C. Minero, D. Vione, Performance and selectivity of the terephthalic acid probe for OH as a function of temperature, pH and composition of atmospherically relevant aqueous media, *J. Photochem. Photobiol. A* 222 (2011) 70–76.
- [16] P. Lorence, *Ethoxyquin solubility: lab project number 4368-95-0177-as-001*, Unpublished Study Prepared By Departement Of Analytical Services, Ricerca Inc., 1996.
- [17] <http://sitem.herts.ac.uk/aeru/iupac/Reports/280.htm.in>.
- [18] G.G. Jayson, B.J. Parsons, A.J. Swallow, Some simple, highly reactive, inorganic chlorine derivatives in aqueous solution. Their formation using pulses of radiation and their role in the mechanism of the Fricke dosimeter, *J. Chem. Soc. Faraday Trans. 1* 1 (69) (1973) 1597–1607.
- [19] http://www.fao.org/fileadmin/templates/agphome/documents/Pests_Pesticides/JMPR/Evaluation99/14Ethoxyquin.pdf.in.
- [20] M. Bodrato, D. Vione, APEX (Aqueous Photochemistry of Environmentally occurring Xenobiotics): a free software tool to predict the kinetics of photochemical processes in surface waters, *Environ. Sci. Process Impacts* 16 (2014) 732–740.
- [21] E. De Laurentiis, M. Minella, V. Maurino, C. Minero, M. Brigante, G. Mailhot, D. Vione, Photochemical production of organic matter triplet states in water samples from mountain lakes, located below or above the tree line, *Chemosphere* 88 (2012) 1208–1213.